Advanced solid elements for sheet metal forming simulation

Journal of Physics: Conference Series **734** (2016) 032128 doi:10.1088/1742-6596/734/3/032128

Advanced solid elements for sheet metal forming simulation

Vicente Mataix[1], Riccardo Rossi[2], Eugenio Oñate[3], Fernando G. Flores[4]

[1 2 3]CIMNE (Centre Internacional de Mètodes Numèrics en Enginyeria), Edificio C1 Campus Nord, UPC, calle Gran Capitán s/n, 08034 Barcelona, Spain
[4] Department of Structures, Universidad Nacional de Córdoba, Casilla de Correo 916, 5000 Córdoba-Argentina, and CONICET, Argentina

E-mail: vmataix@cimne.upc.edu[1], rrossi@cimne.upc.edu[2], onate@cimne.upc.edu[3], fernando.flores@unc.edu.ar[4]

Abstract. The solid-shells are an attractive kind of element for the simulation of forming processes, due to the fact that any kind of generic 3D constitutive law can be employed without any additional hypothesis.

The present work consists in the improvement of a triangular prism solid-shell originally developed by *Flores*[2, 3]. The solid-shell can be used in the analysis of thin/thick shell, undergoing large deformations. The element is formulated in total Lagrangian formulation, and employs the neighbour (adjacent) elements to perform a local patch to enrich the displacement field. In the original formulation a modified right Cauchy–Green deformation tensor ($\bar{\mathbf{C}}$) is obtained; in the present work a modified deformation gradient ($\bar{\mathbf{F}}$) is obtained, which allows to generalise the methodology and allows to employ the **Pull-Back** and **Push-Forwards** operations.

The element is based in three modifications: (a) a classical assumed strain approach for transverse shear strains (b) an assumed strain approach for the in-plane components using information from neighbour elements and (c) an averaging of the volumetric strain over the element. The objective is to use this type of elements for the simulation of shells avoiding transverse shear locking, improving the membrane behaviour of the in-plane triangle and to handle quasi-incompressible materials or materials with isochoric plastic flow.

1. Introduction

Solid-shells have been during the last two decades[4, 5, 6, 7, 8] an important improvement in the shells simulations, providing a reliable simulations and avoiding the problematic that are associated to the kinematics hypothesis and plane stress constitutive laws related to the use of the shell element. The main advantages when using **solid-shell** elements are: a) general 3D constitutive relations; b) large transverse shear can be considered, and considering additional elements along the thickness improve this behaviour; c) there is not need to consider transitions between solid and shell elements (all the elements are solids) ;d) contact forces can be introduced directly in the geometry and in a realistic way without any additional technique, which is specially important for the consideration of friction; e) the element is **rotation-free**, avoiding the storage and computation of this variables;f) in the case where we have non-parallel boundaries this can be modelled correctly.

Most of the existing **solid-shells** are linear hexahedron[4, 5, 6, 7, 8], which have two main disadvantages; the first one is the *hourglass* effect; the second problematic is the meshing of the plane, due to the fact that meshing quadrilateral is less performant than triangles. For this

reasons the triangular prisms (wedges) could be considered an interesting alternative, specially for the second problem mentioned, but this kind of geometry is not exempt of problematic, owing to the low order of interpolation of the geometry; this can be solved with the consideration of the neighbours elements, in consequence the element becomes quadratic in the plane solving this last problem.

The element has been implemented into *Kratos*[16], the in-home **FEM-Multiphycis** open-source code, implemented in C++ with parallilization capabilities. The pre/post-process of all the presented examples haven been processed with *GiD*, the *CIMNE* software for pre and post porcessing. The content of this proceeding will be the following one: 1) A resume of the theory concerning to the element is presented, focusing in what has been improved from the original element[2, 3] , 2) Some test cases are presented to show the good performance of the element. Additionally, more examples of application of the new solid-shell elements will be shown in the oral presentation in the congress.

2. Theory

For the aim of brevity we will focus in the improvements introduced in the original formulation from *Flores*[2, 3], and we will address to the original material for additional information.

2.1. Pull-Back and Push-Forward (Extension of the formulation)

The formulation presented until now is broadly the formulation already presented in the works of *Flores*[1, 2, 3], the main step forward of this work is the extension of the formulation. As we have seen the formulation presented allows us to obtain a modified left *Cauchy* tensor $\bar{\mathbf{C}}$. With this tensor we are able to obtain strains in a traditional way, *g.e* with *Green-Lagrange*, but we are unable to work with the **Pull-Back** and **Push-Forward** operations.

In order to perform these operations we need the deformation gradient $\mathbf{F}$, or in our case $\bar{\mathbf{F}}$ owing to we are working with a modified right *Cauchy* tensor $\bar{\mathbf{C}}$. Obtain one from another is not a trivial operation, and we must consider additional assumptions to obtain our modified deformation gradient. In a standard formulation to obtain the deformation gradient $\mathbf{F}$ we compute (1) from the material displacement gradient tensor $\nabla_{\mathbf{X}}\mathbf{u}$, $\mathbf{C}$ can be obtained easily from here.

$$\mathbf{F} = \nabla_{\mathbf{X}}\mathbf{u} + \mathbf{I} \rightarrow \mathbf{C} = \mathbf{F}^T\mathbf{F} \tag{1}$$

We will present now (2a) the polar decomposition of $\mathbf{F}$, which will be the key idea considered to obtain $\bar{\mathbf{F}}$. In this decomposition $\mathbf{R}$ represents the *proper orthogonal tensor* and $\mathbf{U}$ is the *right stretch tensor*. The *right stretch tensor* can be computed from the square root of the right *Cauchy* tensor. The only remaining component needed to compute the $\bar{\mathbf{F}}$ will be the modified *proper orthogonal tensor* where we will take the assumption of $\bar{\mathbf{R}} = \mathbf{R}$. The computation of this $\bar{\mathbf{F}}$ is summarized in (2b).

$$\mathbf{F} = \mathbf{R}\mathbf{U} \text{ and } \mathbf{U} = \sqrt{\mathbf{C}} \tag{2a}$$

$$\bar{\mathbf{F}} = \mathbf{R}\bar{\mathbf{U}} \begin{cases} \mathbf{C} = \mathbf{F}^T\mathbf{F} \rightarrow \mathbf{U} = \sqrt{\mathbf{C}} \rightarrow \mathbf{R} = \mathbf{F} \cdot \mathbf{U}^{-1} \\ \bar{\mathbf{U}} = \sqrt{\bar{\mathbf{C}}} \end{cases} \tag{2b}$$

With the modified $\bar{\mathbf{F}}$ we are able to compute the **Pull-Back** and **Push-Forward** operations, which allow us to to have an unified description between the *Eulerian* and *Lagrangian* tensors. In (3) we can appreciate some examples, where a **Push-Forward** by $\mathbf{F}$ of the *Lagrangian* vector $d\mathbf{X}$ to the current configuration gives the *Eulerian* vector $d\mathbf{x}$, and vice-versa with the **Pull-Back** operation. These concepts provide us a mathematically consistent method for define the time derivatives of the tensors, called **Lie-derivatives**. Considering all this, the operations can be considered for example to obtain a formulation of **hyperelastic-plastic** constitutive model based on the multiplicative decomposition of the deformation gradient, for more information consult[12].

$$d\mathbf{x} = \mathbf{F} \cdot d\mathbf{X} \equiv \phi_* d\mathbf{X} \text{ and } d\mathbf{X} = \mathbf{F}^{-1} \cdot d\mathbf{x} \equiv \phi^* d\mathbf{x} \tag{3}$$

3. Test cases

The following test examples here presented shown the good performance and behaviour of the element. The main references of this results are taken from the original paper from *Fernando Flores*[2, 3], but many of the results are taken too from[15] a work with the most significatives benchmarks for test the shell behaviour. All the test results can be found in Figure 1.

- **Cook's membrane test:** Figures 1a and 1b represent the behaviour of the *Cook's* membrane, respectively elastic and elasto-plastic, both obtained considering an implicit scheme. The results present even less than the reference[3] locking for the elastic case and similar behaviour for the elasto-plastic case.
- **Open ended cylindrical shell test:** The results (Figure 1c) agrees with the solution from [15].
- **Slit test:** Can be seen (Figure 1d) that with the refinement of the mesh the solution tend to the correct one [15].
- **Panel test:** The panel test is a common test which presents a highly non-linear behaviour, and it is necessary an arc-length to compute. The results obtained, Figures 1e and 1e, show a clearly agreement with the reference [15].
- **Sphere test:** The Figure 1g presents the results obtained for the semi-spherical shell with a ratio $R/t = 1000$, which agrees with the results from [15].
- **Cone-shell test:** This problem is commonly considered to study the combination both plasticity and geometrical non-linearity, the results shown in Figure 1h differ from [14], but with a close behaviour.

4. Acknowledgments

I want to mention the support of the *Generalitat de Catalunya* which is funding my PhD with the grant *Agaur*.

5. References

[1] Flores F G 2013 *Mecánica Computacional* **XXXII** 63–87
[2] Flores F G 2013 *Computer Methods in Applied Mechanics and Engineering* **253** 274–286
[3] Flores F G 2013 *Computer Methods in Applied Mechanics and Engineering* **266** 81–97
[4] Dvorkin E N and Bathe K J 1984 *Engineering computations* **1** 77–88
[5] Hauptmann R and Schweizerhof K 1998 *International Journal for Numerical Methods in Engineering* **42** 49–69
[6] de Sousa R J A, Cardoso R P R, Valente R A F, Yoon J W, Grácio J J and Jorge R M N 2005 *International journal for numerical methods in engineering* **62** 952–977
[7] Klinkel S, Gruttmann F and Wagner W 2006 *Computer Methods in Applied Mechanics and Engineering* **195** 179–201
[8] Parente M, Valente R F, Jorge R N, Cardoso R and de Sousa R J A 2006 *Finite Elements in Analysis and Design* **42** 1137–1149 ISSN 0168-874X
[9] Oñate E and Flores F G 2005 *Computer Methods in Applied Mechanics and Engineering* **194** 2406–2443 ISSN 0045-7825 computational Methods for Shells
[10] Flores F G and Oñate E 2005 *Computer Methods in Applied Mechanics and Engineering* **194** 907–932 ISSN 0045-7825
[11] Flores F G and Oñate E 2011 *Finite Elements in Analysis and Design* **47** 982–990
[12] Belytschko T, Liu W K, Moran B and Elkhodary K 2014 *Nonlinear Finite Elements for Continua and Structures* 2nd ed (Wiley)
[13] Olovsson L, Unosson M and Simonsson K 2004 *Computational Mechanics* **34** 134–136 ISSN 1432-0924
[14] Klinkel S, Gruttmann F and Wagner W 2006 *Computer Methods in Applied Mechanics and Engineering* **195** 179–201 ISSN 0045-7825
[15] Sze K, Liu X and Lo S 2004 *Finite Elements in Analysis and Design* **40** 1551–1569 ISSN 0168-874X
[16] Kratos Homepage URL `http://www.cimne.com/kratos/`

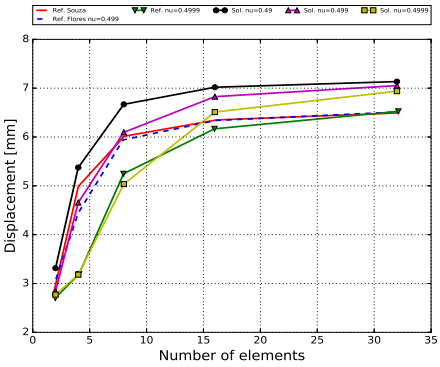

(a) Elastic Cook's membrane

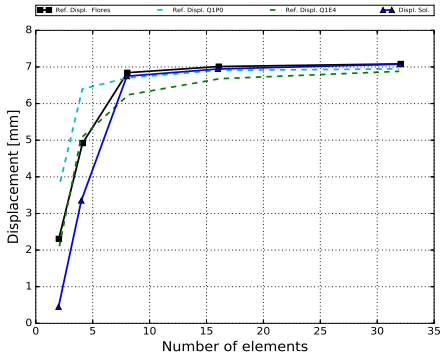

(b) Elasto-plastic Cook's membrane

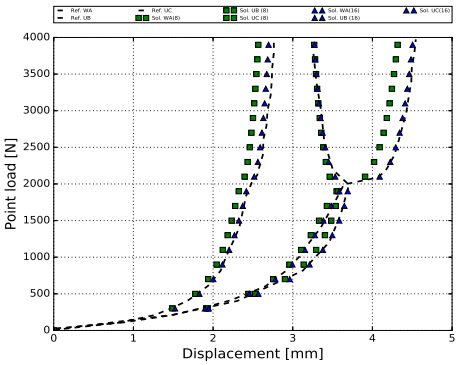

(c) Load-deflection for the open-ended cylindrical shell

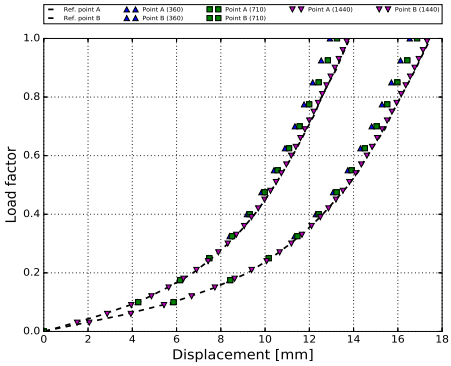

(d) Load-deflection for the slit test

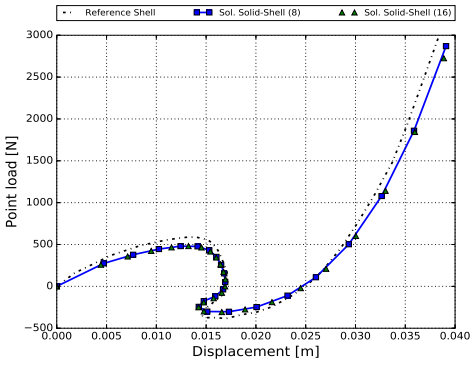

(e) Panel load-deflection $h = 6.35mm$

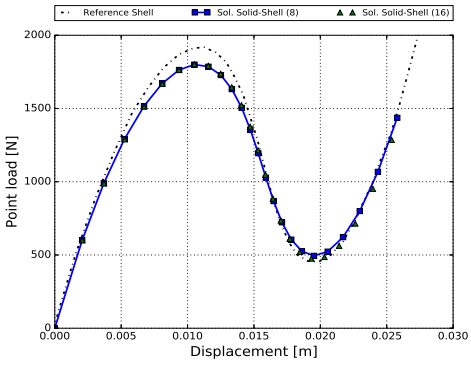

(f) Panel load-deflection $h = 12.7mm$

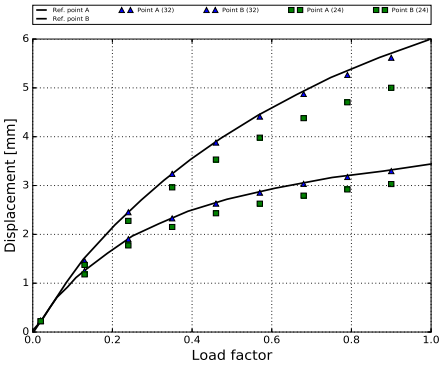

(g) Sphere load-deflection $R/t = 1000$

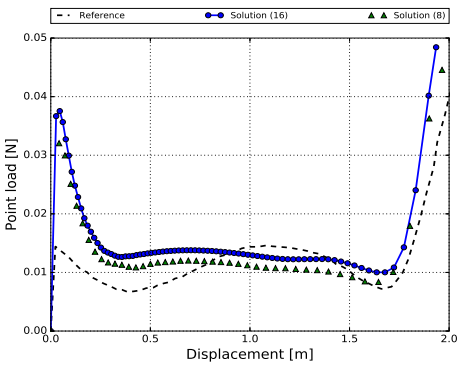

(h) Load-deflection curve for the cone-shell test

Figure 1: Resume of the tests results